Regional Studies in Marine Science 6 (2016) 109–123

Contents lists available at ScienceDirect

Regional Studies in Marine Science

journal homepage: www.elsevier.com/locate/rsma

A management oriented 1-D ecosystem model: Implementation in the Gulf of Trieste (Adriatic Sea)

Giulia Mussap [a,*], Marco Zavatarelli [b], Nadia Pinardi [b], Massimo Celio [c]

[a] CIRSA, University of Bologna, Ravenna, Italy
[b] DIFA, University of Bologna, Bologna, Italy
[c] ARPA Friuli Venezia Giulia, Palmanova, Udine, Italy

HIGHLIGHTS

- The BFM–POM 1D system successfully replicated the observed seasonal variability.
- The microbial food web dominates the Gulf of Trieste trophic structure.
- External inputs variability can change the trophic web structure.
- A first step for developing a modelling system supporting environmental management.

ARTICLE INFO

Article history:
Received 29 September 2015
Received in revised form
23 March 2016
Accepted 25 March 2016
Available online 7 April 2016

Keywords:
Biogeochemistry
Modelling
Ecosystem management
Trophic structure
Adriatic Sea
Gulf of Trieste

ABSTRACT

In this paper a coupled physical–biogeochemical one-dimensional numerical model (BFM–POM 1D) was implemented in the Gulf of Trieste, (northern Adriatic Sea) and its structure was tested in order to evaluate its usability as a tool to support coastal management and planning. The evaluation concerned the ability of the model to reproduce the main trophic pathways, as well as their temporal variability, in terms of seasonal variations. The ecosystem structure comprised three phytoplankton groups, four zooplankton groups, one bacterial group, and a simple benthic return in order to parametrise benthic processes. The dynamics and interactions between groups were studied, as well as the model's sensitivity to different trophic web configurations. Results showed that the model was capable of replicating the behaviour of seasonal vertical profiles of the major biogeochemical elements, and the prevalence of the microbial food web shaping the trophic chain in the Gulf of Trieste. The model also responded to strong forcings at the surface and different trophic arrangements, thus providing initial evidence of its potential as a scientific tool aimed at marine coastal management.

1. Introduction

The biogeochemical state of the ocean depends on biogeochemical cycling and on fluxes across the ocean boundaries (land, atmosphere and sea floor, Doney, 2010). In shallow coastal waters (the most productive regions of the global ocean), the role of such fluxes is amplified. These areas therefore play a fundamental role in shaping global biogeochemical dynamics and trophic interactions. However, they are also very vulnerable and subject to strong anthropogenic pressure that significantly affects the major marine biogeochemical cycles.

In order to define and implement ecosystem-based options and strategies, a deep understanding of the functioning and dynamics of the ecosystem is required (Curtin and Prellezo, 2010). Observational and modelling tools can be used to assess the current state of the system, its main ecosystem attributes exposed to the joint action of direct and indirect anthropogenic pressure, and subsequently to explore the effects related to the implementation of a specific management plan. Thus, the modelling tool (supported by an adequate observational base), plays a critical role to envision how the major biogeochemical fluxes could change and/or modify their interactions in response to the drivers (e.g. climatic and/or anthropogenic) of change.

In 2003 Vichi et al. implemented the biogeochemical model ERSEM (Baretta et al., 1995), from which the BFM was later developed, in three sites in the northern Adriatic. Apart from our overall aim, the major differences of our study with respect to

* Corresponding author.
E-mail address: g.mussap@sincem.unibo.it (G. Mussap).

http://dx.doi.org/10.1016/j.rsma.2016.03.015

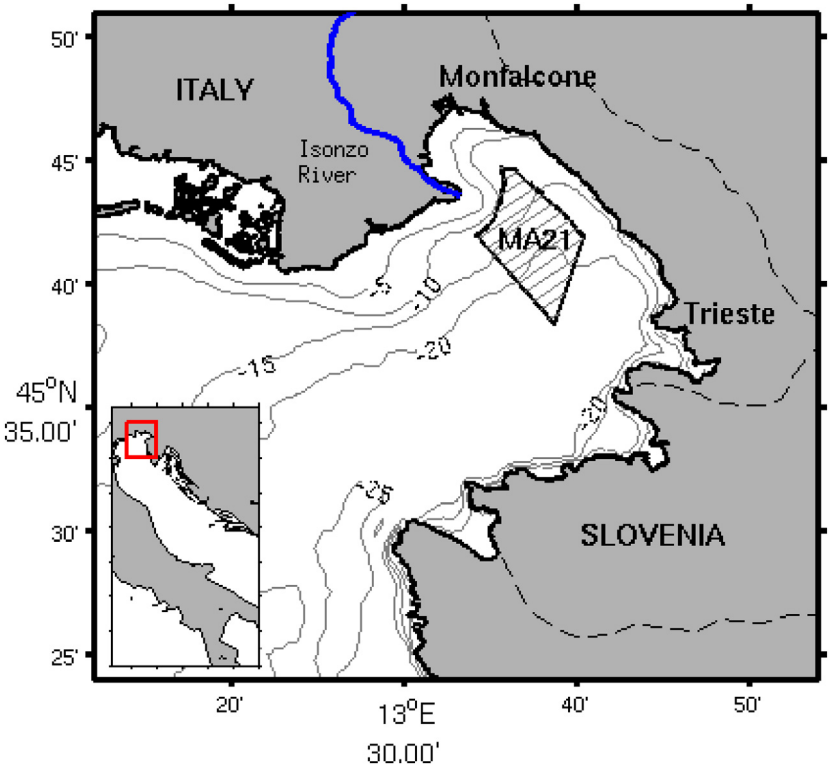

Fig. 1. Map and bathymetry (in metres) of the Gulf of Trieste with location of the implementation area MA21.

Vichi et al. (2003) were the use of the latest version of BFM and the implementation of the hydrodynamical model in a diagnostic mode. The aim of this paper is to establish and test the structure of a coupled (physical–biogeochemical) one-dimensional numerical model (BFM–POM 1D) in order to evaluate its suitability as a tool for testing environmental management options for coastal oceans. We studied the ecosystem structure of lower trophic levels (primary producers and consumers) and their interactions by investigating the sensitivity of the simulated fluxes with respect to different configurations of the trophic web and to a stronger surface forcing. Mechanistic experiments were thus carried out and results are discussed with emphasis on the changes in the fluxes determined by such configurations. The experiments comprised the alternating activation/deactivation of the herbivorous and microbial foodwebs and the amplification of surface nutrient forcing. A qualitative study of system reactions was carried out in order to understand the extent to which different compartments determine carbon fluxes and biogeochemical cycling.

As an initial testbed, the model was implemented and tested in the Gulf of Trieste (northern Adriatic Sea). The reason for this choice is twofold: the Gulf has been the focus of previous modelling efforts (Vichi et al., 2003; Butenschon et al., 2012) and a rich dataset is available, thus enabling the definition of a valid and reliable hydrological climatology.

2. Materials and methods

2.1. Model implementation

Bordering Italy and Slovenia on the northern-east coast of the Adriatic sea (Fig. 1), the Gulf has an average depth of 20 m. The whole area is strongly affected by river runoff, especially along the shallow northwestern coast (Isonzo River). The implementation area was chosen on the basis of the Gulf's macroareas identified by the regional environmental agency (ARPA-FVG), on the basis of the distance from the coast, geomorphology, hydrological characteristics (water column stability) (Butenschon, 2012) and freshwater inputs. Following the definition of the area types, the hydrological bodies were identified on the basis of the environmental status highlighted in previous monitoring campaigns, the limits of the protected areas, and the pressures influencing the achievement of the quality objectives.

The model implementation area is code-numbered MA21 and is situated in the centre of the Gulf (Fig. 1). Monitoring data for to the whole area were analysed and used to set initial conditions, surface boundary conditions, and to validate the model's performance.

The hydrological features of the Gulf show a very large interannual and seasonal variability (Vichi et al., 2003). Although the circulation is very variable, the Gulf is generally characterised by a cyclonic circulation mainly driven by freshwater inputs by the Isonzo and Po rivers, while tidal currents play a small role in the circulation (Guarnieri et al., 2013). The biogeochemical characteristics of the Gulf of Trieste are also subject to a significant interannual variability depending mostly on the variability of the land based nutrient inputs conveyed to the sea above all by the discharge of the Isonzo river and by anthropogenic pressure. This gives rise, for instance, to a wide qualitative and quantitative variability in the phytoplankton population structure (Mozetic et al., 1998, 2010; Tedesco et al., 2007). Nonetheless, generally speaking the Gulf, as with most of the Mediterranean, is P-limited. As a result of such physical features, primary production is characterised by a winter bloom and by high concentrations near the seabed during spring and summer.

2.2. Coupled numerical model set-up

The one-dimensional coupled numerical model used is composed of the one-dimensional version of the Princeton Ocean Model (POM) (Blumberg and Mellor, 1987) and the Biogeochemical Flux Model (BFM) (Vichi et al., 2007).

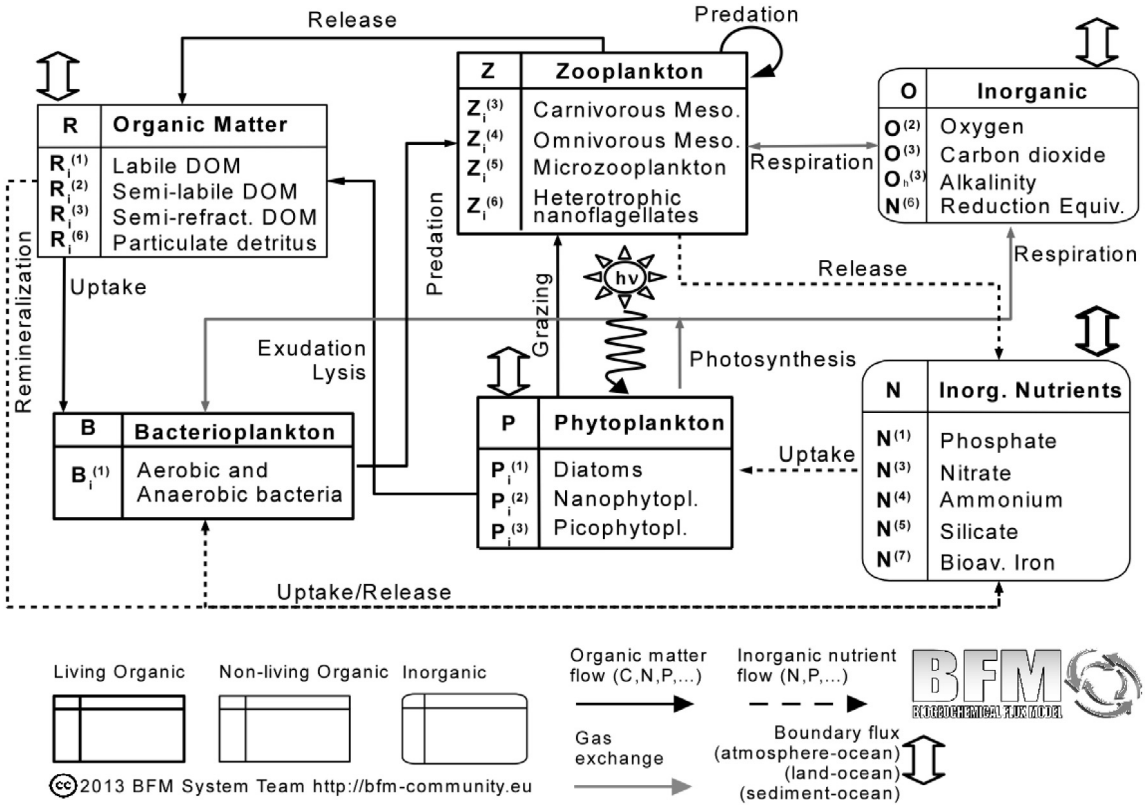

Fig. 2. General overview of the matter fluxes between the BFM state variables. Square boxes represent the model functional groups exchanging Carbon (C), Nitrogen (N), Phosphorus (P), Silicon (Si) and Oxygen (O). Organic matter (C, N, P, Si) flows are indicated by solid black arrows; N, P and Si nutrient uptake/remineralisation flows are represented by the dashed black arrows. Solid grey arrows mark the gas C (Carbon dioxide) and O flows. Purely biochemical processes are indicated by the dashed grey arrows. Small double arrows above the boxes mark boundary (water–atmosphere and water–sediment) flow. After Vichi et al. (2007).

The open source BFM (http://bfm-community.eu/) describes the physiological and population processes of lower trophic levels in the marine environment. Biota is described by means of three main functional groups: producers, decomposers and consumers, each one defined by internal constituents: carbon, nitrogen, phosphorous, oxygen and (in the case of diatoms) silicon (Vichi et al., 2007). The model includes three phytoplankton groups (diatoms, nanophytoplankton and picophytoplankton), four zooplankton groups (carnivorous mesozooplankton, omnivorous mesozooplankton, microzooplankton and heterotrophic nanoflagellates) and one bacterial group. Trophic and chemical interactions are represented through chemical functional families (CFFs) and Living Functional Groups (LFGs) (Vichi et al., 2007). CFFs are defined as the inventory of a certain biogeochemical element contained in complex living and non-living components, and are divided into three main groups: non-living organic, living-organic and inorganic. These groups are measured based on the major chemical elements (C, N, P, Si, O) or on molecular weight units as with chlorophyll. The living organic group represents the LFGs, which are made up of producers (phytoplankton), consumers (zooplankton) and decomposers (bacteria). The dynamics of each of these are described by population processes (growth, migration, mortality) and physiological processes (photosynthesis, ingestion, respiration, excretion, egestion). Regarding the benthic compartment, a simple benthic return was used (see Table A.7). This choice was made in order to simplify an already fairly complex system. Since the focus was directed towards the interactions in the pelagic realm, a simple benthic return was considered initially sufficient to support major biogeochemical dynamics. In fact, this configuration was already found to be a valid replacement to complex benthic dynamics (Vichi et al., 2003). Fig. 2 shows the biogeochemical model structure and a detailed description of each model component can be found in Appendix A.

POM is a primitive equation ocean circulation model formulated in sigma coordinates that computes diffusivity by means of a second-order turbulence closure scheme proposed by Mellor and Yamada (1982). We used the one-dimensional version of the model implemented with 30 σ layers ($\sigma = z/H$) logarithmically distributed near the bottom and surface. In this implementation, the bottom depth is $H = 16$ m, corresponding to a typical depth for area MA21. At each model timestep, the hydrodynamics computed by POM provides the BFM with information on the physical environment. The coupled model combines physics with biology to compute the temporal rate of change of a generic biogeochemical variable (expressed in terms of concentration, see Appendix A). The two components of the modelling system are coupled online using the source-splitting method described in Butenschon et al. (2012).

Following Bianchi et al. (2006) we used POM in diagnostic mode: the climatological time dependent (monthly varying) temperature and salinity vertical profiles, obtained from data, were prescribed, while the vertical profiles of vertical diffusion coefficients were computed by the model through the (Mellor and Yamada, 1982) second order turbulent closure scheme. The coefficients are used to compute the vertical profiles of the BFM state variables. The use of the "diagnostic" mode eliminates possible drifts in temperature and/or salinity due to the use of a "non zero" surface heat and/or mass surface fluxes or to the lack of a proper parametrisation of the lateral advective fluxes, which are by necessity not contained in a one-dimensional model implementation. The use of the diagnostic mode with climatological data, provides a stable (non-drifting) annual cycle of the vertical density structure, which is particularly suitable when using the numerical model to evaluate possible options of environmental management. Clearly, the reliability of the simulations relies on the quality of the assembled climatology. Therefore, a 1-D modelling system relying on the

Table 1
Summary of available measured data, source, period and application. Climatologies were used as model forcings and for validation purposes. The model derives the Photosynthetic Available Radiation (PAR) from the total solar radiation.

Variable	Units	Period	Climatology
Forcings			
Temperature	°C	2000–2011, 2013	Monthly
Salinity	psu	2000–2011, 2013	Monthly
Wind stress	N m^{-2}	2000–2013	Monthly
Solar radiation	W m^{-2}	2000–2013	Monthly
Inorganic suspended matter	mg m^{-3}	1997–2000	Seasonal
Phosphate	mmol m^{-3}	1998–2001	Monthly
Nitrates	mmol m^{-3}	1998–2001	Monthly
Ammonium	mmol m^{-3}	2000–2001	Monthly
Silicate	mmol m^{-3}	2009–2012	Monthly
Validation data			
Phosphate	mmol m^{-3}	1998–2001	Seasonal
Nitrates	mmol m^{-3}	1998–2001	Seasonal
Ammonium	mmol m^{-3}	2000–2001	Seasonal
DOC	mg m^{-3}	2000–2001	Seasonal
POC	mg m^{-3}	2000–2001	Seasonal
PON	mmol m^{-3}	2000–2001	Seasonal
Oxygen	mmol m^{-3}	2000, 2002–2011, 2013	Seasonal
Chlorophyll-a	mg m^{-3}	2000–2011, 2013	Seasonal

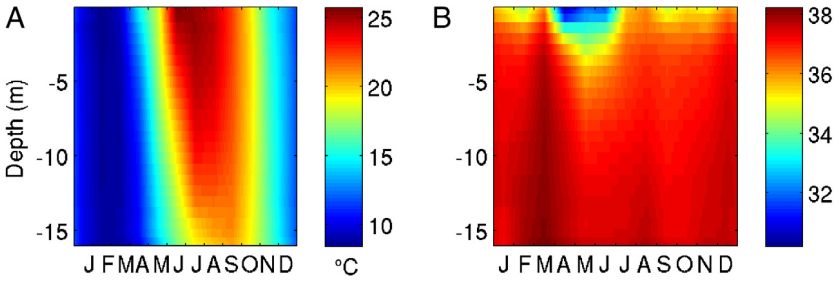

Fig. 3. Temperature (A) and salinity (B) monthly climatological profiles calculated from available *in situ* data (Table 1) fed to the model and interpolated on its time step.

diagnostic description of the density vertical structure entails the implementation in a hydrological "data-rich" area such as areas where observing systems are in place. The hydrological data (temperature and salinity profiles) used to compose the prescribed climatology originate from the monitoring activities carried out in the MA21 by ARPA-FVG and OGS from 2000 to 2013 (see Table 1).

The climatological annual cycles of the vertical temperature and salinity are shown in Fig. 3(A) and (B), respectively. They show a seasonal cycle characterised by well-mixed conditions in the winter and by vertical thermal stratification in the summer. Surface salinity is affected by pulses of freshwater mostly due to the Isonzo river discharging in the Gulf, while below the surface, there are periodical increases in the salinity value, most probably due to the ingression of saltier water in the Gulf (Malacic and Petelin, 2009).

2.3. Forcing functions and initial conditions

The use of the diagnostic mode for the physical component of the modelling system, entails specifying the surface wind stress as the only surface forcing function. The annual, monthly-varying, climatology used here was obtained from the 6-hour ECMWF ERA-interim reanalysis (Berrisford et al., 2009) for 2000–2013 (Fig. 4(A) and Table 1). Wind stress is highest and more variable (higher standard deviations) during winter and autumn, reflecting the prevalence of the typical strong Bora (northeasterly) and Scirocco (southeasterly) winds, respectively (Kourafalou, 1999; Zavatarelli et al., 2002). Winds are weaker during spring and summer.

The daily surface incident shortwave radiation necessary to force the BFM primary production module also originates from the ECMWF data (Fig. 4(B) and Table 1). The ECMWF solar radiation arriving at the sea surface penetrates the vertical column as photosynthetically available radiation (PAR). The PAR vertical profile is then calculated using the Lambert–Beer equation (see Appendix A) using a vertical extinction coefficient composed of the time-dependent prognostic phytoplankton and particulate detritus concentrations. In addition extinction is used depending on the inherent optical properties of the seawater and the concentration of inorganic suspended matter (ISM), whose seasonally averaged profiles originate from direct measurements in area MA21 (Fig. 4(C), Table 1). Observations were collected monthly over the period 1997–2000 (Vichi et al., 2003). The inconsistency of the time period used between other physical forcings (2000–2013) and ISM (1997–2000) is due to the scarce climatological information available concerning seasonal mean concentrations. This degree of uncertainty was taken into account in the general performance of the model.

In order to parametrise the external (land based) nutrient input, we defined a surface nutrient flux by relaxing the surface value to a monthly varying climatology of phosphate, nitrate, ammonia and silicate (Table 1, Fig. 4(D)). The surface boundary conditions used are detailed in Appendix A (see Eq. (A.5)).

The initial climatological conditions for biogeochemical pelagic components were set for a vertically-homogeneous profile consistent with the observed winter concentrations. The benthic system was initialised with an educated guess regarding the detrital organic matter based on the literature (Giordani et al., 1992). Tests to determine the spin up period showed that a five year integration period yielded a repeating seasonal cycle after three years. Therefore, results were analysed from the fifth year of simulation, where the first four years were considered as the specific spin-up time necessary for the model to find equilibrium.

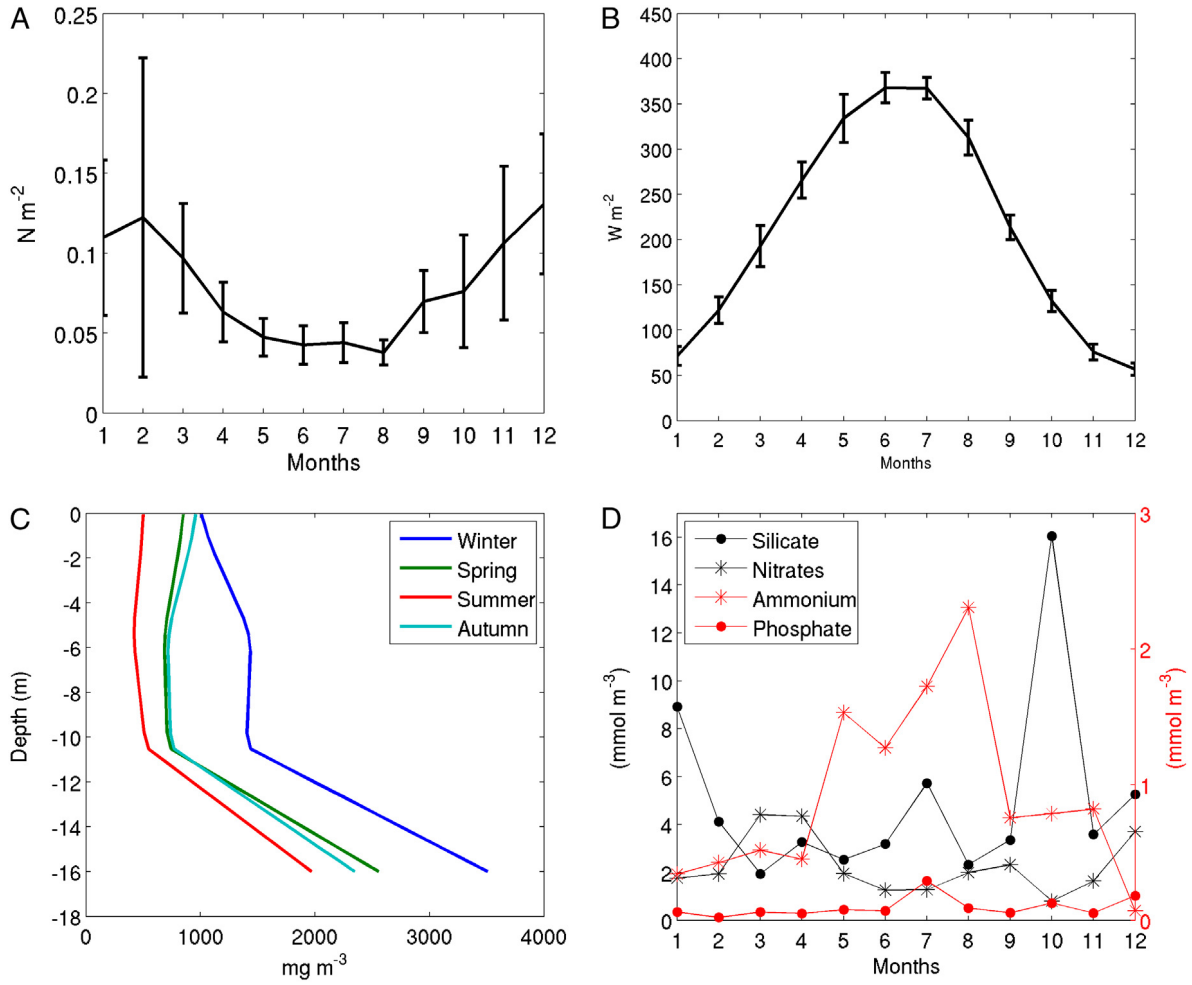

Fig. 4. Climatological forcing functions (A) Wind stress monthly varying climatology from the 6-h ECMWF ERA-interim reanalysis relative to the period 2000–2013. (B) Solar radiation daily varying climatology from the 6-h ECMWF ERA-interim reanalysis relative to the period 2000–2013. (C) Inorganic Suspended Matter (ISM) monthly varying climatological concentrations for the period 1997–2000. (D) Surface monthly varying climatological concentrations of nutrients for the period 1998–2012 (see Table 1).

2.4. Validation data

Tables 1 and 2 summarise the biogeochemical observations used to validate the model results at the seasonal climatological level (winter: January to March, spring: April to June, summer: July to September, autumn: October–December).

The biogeochemical data used to force the model are scarce but temporally consistent with the profiles used for validation. Chlorophyll and oxygen validation profiles were computed from a longer time period compared to the other variables, resulting in a relatively more robust seasonal climatology.

Seasonal climatological vertical profiles were computed from the available data, along with the corresponding standard deviations (unless lack of data prevented its calculation). Seasonal profiles and corresponding standard deviations are shown in Fig. 5 for comparison with the model results.

2.5. Numerical experiments

Mechanistic experiments were performed in order to understand the low level trophic ecosystem structure and test the capacity of the model as a scientific tool aimed at tackling coastal management issues. As Kiørboe (2008) and Azam and Long (2001) argue, our knowledge on the lower level trophic system is rudimentary and there is the need for a mechanistic understanding of the system. With the mechanistic methodology we intend to modify trophic interactions in order to demonstrate the importance of the different functional ecosystem components in the organic carbon flux dynamics.

The overall response of the model was assessed. In particular, we evaluated the sensitivity of the system to different levels of nutrient forcing as well as to the presence/absence of a full herbivorous chain and microbial loop in the simulated ecosystem. Table 3 presents the simulations carried out.

The BASE experiment was carried out with the full BFM, and the results were used to validate the modelling system. With the MICRO and HERB experiments, the role of the two trophic structures – classical herbivorous food chain versus microbial food web – were studied. The aim of the experiments was to understand to what extent the microbial web, previously proven to be key to certain fluxes and dynamics (Fonda Umani and Beran, 2003), shapes the trophic structure in relation to the herbivorous food web. The two food chains were isolated one at a time, and details of the resulting trophic structures are provided below. The HERB experiment configuration simplifies the system thus making it a more classical NPZD model, where microbial dynamics are absent and the system is closed by a constant remineralisation rate. Organic matter remineralisation is thus computed by introducing a constant remineralisation rate, which is not temperature dependent, while the grazing pressure on the primary producers is entirely dependent on the herbivorous mesozooplanktonic group.

Finally, experiment BASE × 5 examined the model's sensitivity to different surface nutrient forcing scenarios. Testing the model's response to different drivers is fundamental in order to

Table 2
Number of samples per biochemical variable divided by season in the depth intervals indicated. For chlorophyll and oxygen, numbers refer to 1 m vertical resolution casts.

Variable	Depth (m)	Winter Jan–Mar	Spring Apr–Jun	Summer Jul–Sep	Autumn Oct–Dec
Chlorophyll	Casts	62	66	65	66
Oxygen	Casts	56	63	60	60
Nitrates	0–3	19	17	15	13
	3–6	5	12	9	3
	6–9	3	4	2	3
	9–12	11	7	7	5
	12–15	0	7	5	3
	15–18	0	0	6	0
Phosphate	0–3	10	11	11	8
	3–6	3	8	5	2
	6–9	0	2	1	2
	9–12	7	5	5	4
	12–15	0	3	3	1
	15–18	0	0	3	0
Ammonium	0–3	8	6	6	4
	3–6	2	4	4	1
	6–9	2	2	1	1
	9–12	4	2	2	1
	12–15	0	4	2	2
	15–18	0	0	3	0
DOC	0–3	7	6	6	4
POC	3–6	2	4	4	1
PON	6–9	2	2	1	1
	9–12	4	2	2	1
	12–15	0	4	2	2
	15–18	0	0	3	0

Table 3
Summary of numerical experiments: BASE (complete BFM), MICRO (only microbial food web), HERB (only herbivorous food web) and BASE × 5 (multiplies by 5 the surface nutrient forcing). P1: diatoms, P2: nanophytoplankton, P3: picophytoplankton, Z3: carnivorous, Z4: omnivorous mesozooplankton, Z5: microzooplankton, Z6: heterotrophic, B1: bacteria.

Experiment	Herbivorous (P1, P2, Z3, Z4)	Microbial (P3, B1, Z5, Z6)	Surface nutrients
BASE	Yes	Yes	clim.
MICRO	No	Yes	clim.
HERB	Yes	No	clim.
BASE × 5	Yes	Yes	clim. × 5

provide consistent predictions regarding changes in the major biogeochemical fluxes. In this experiment, the surface nutrient data fed to the model were multiplied by five, thus dramatically increasing the nutrient concentrations.

3. The BASE experiment and its sensitivity

3.1. Seasonal validation

The BASE experiment was designed to validate the model results from the full blown BFM. Simulated seasonally averaged vertical profiles of chlorophyll, oxygen, phosphate, nitrates, dissolved organic carbon (DOC), particulate organic carbon (POC) and particulate organic nitrogen (PON) were compared to the corresponding seasonal profiles observed (see Table 1).

The simulated and observed seasonal profiles are compared in Fig. 5. The results indicate that the model replicates chlorophyll and oxygen seasonal variability within one standard deviation (Fig. 5, rows A and B respectively). Seasonal profiles always fall within the observed standard deviation, except for the simulated spring chlorophyll profile, which is underestimated. The simulated vertical profiles of phosphate and nitrates (Fig. 5, rows C and D respectively) lie close to the mean or fall within one standard deviation of the specific observations. However, the simulated seasonal variability of ammonium (Fig. 5, row E) for winter and spring is characterised by a concentration increase in depth which does not match the observed data. This overestimation is certainly one aspect of the model's configuration that requires careful attention. The constant benthic remineralisation rate and the absence of a complex benthic chamber could be the reason behind this mismatch.

The simulated vertical profiles of DOC, POC and POM (Fig. 5, rows F, G, H respectively) show points of agreement and disagreement with observations. In the majority of the observed vertical points, the data were so scarce that it was not possible to compute the standard deviations, and an evaluation of the model's reliability is therefore difficult. Although simulated concentrations are underestimated, DOC seasonal profiles show a qualitative agreement with observations (homogeneous vertical profiles in winter and autumn, and concentrations decreasing in depth in spring and summer). On the other hand, the POC and POM simulated profiles show vertical structures that differ from the vertical profiles observed, with a nearly constant increase from the surface to the bottom. Concentration magnitudes however fell within the bulk values. Again, the mismatch in the vertical structure could be connected to the simplified benthic boundary condition, which does not account for major benthic processes.

3.2. Sensitivity of the forcings

Given the temporal non-homogeneity in the datasets used to define the model forcings (see Table 1), a sensitivity test was

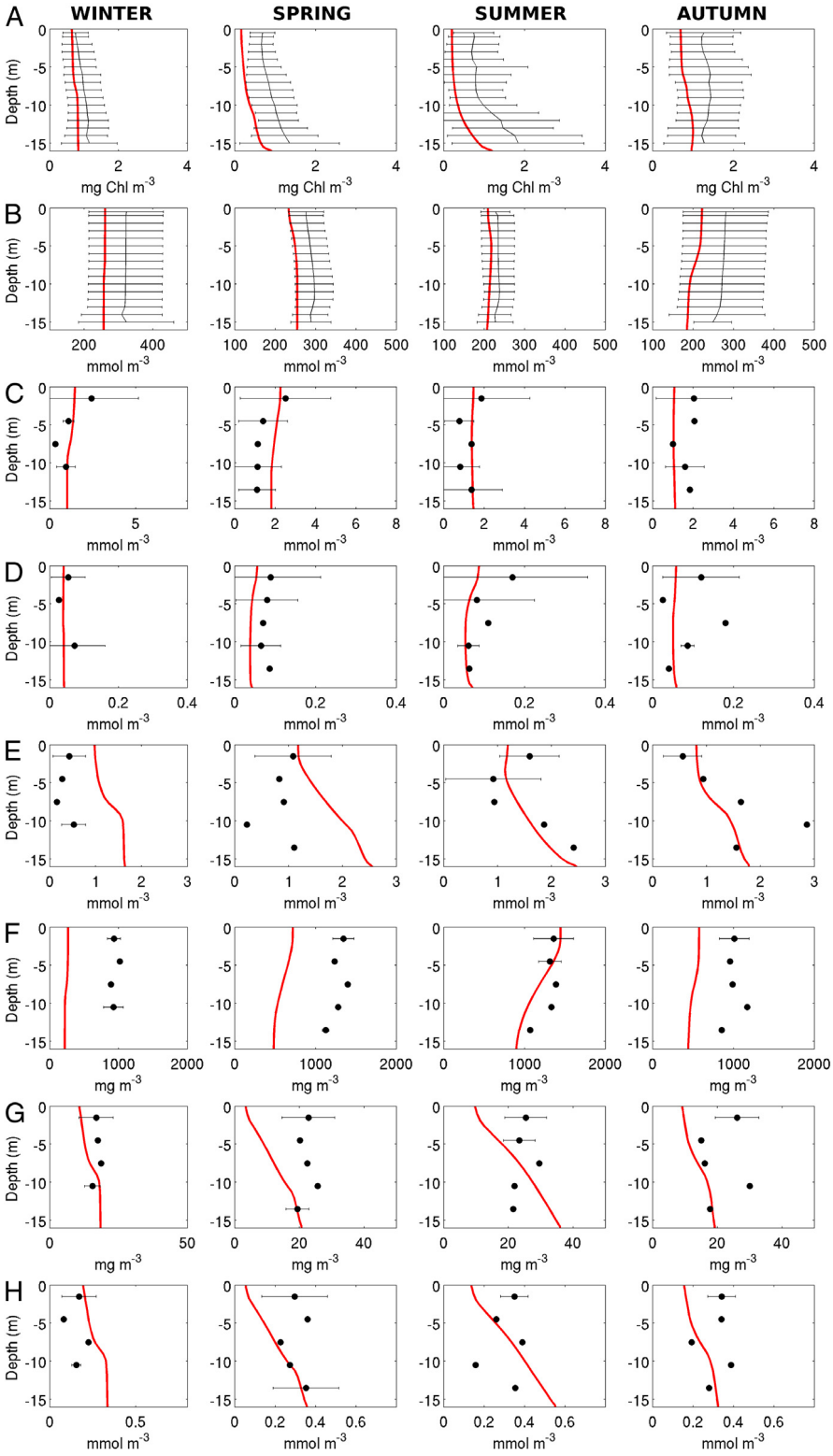

Fig. 5. Model and data comparison for (A) chlorophyll, (B) oxygen, (C) nitrates, (D) phosphate, (E) ammonium, (F) DOC, (G) POC and (H) PON as climatological seasonal profiles for site MA21. The continuous red line is the simulated mean seasonal profile, while observations are plotted as seasonal means with the standard deviation (where data allows it). (For interpretation of the references to colour in this figure legend, the reader is referred to the web version of this article.)

carried out using different time averaged surface biochemical and physical fields. It was decided to force the model only with temperature, salinity, wind stress and solar radiation from the overlapping period, 2000–2001. Biogeochemical seasonal vertical profiles were compared to the BASE experiment and the results are shown in Figure S1. This sensitivity experiment showed that the average forcings of temperature, salinity, solar radiation and wind stress for 2000–2001 produced seasonal profiles that fell within a 25% difference compared to those obtained in the BASE experiment.

The results show that the different time-averaged forcings produced qualitatively the same ecosystem response. The largest dif-

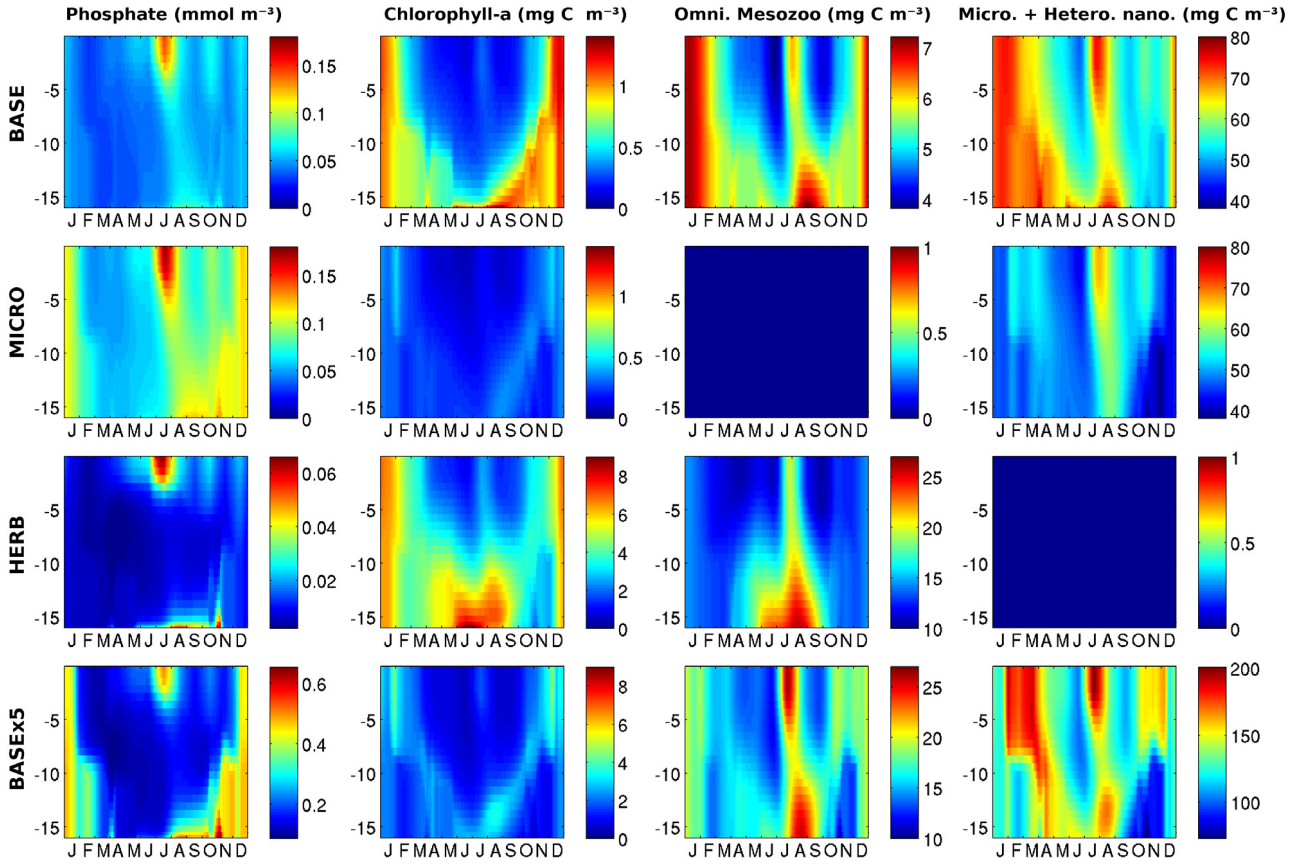

Fig. 6. Hovmöller plots of modelled results of phosphate, chlorophyll-a, omnivorous mesozooplankton and microzooplankton with heterotrophic nanoflagellates for the BASE, MICRO, HERB and BASE × 5 experiments (top to bottom). Depth on the *y*-axis, months on the *x*-axis. Note the differences in scales.

ferences were in oxygen and nitrates in summer, and in ammonia in winter and autumn due to the sensitivity to chemical rates to different temperature conditions. We believe that such differences do not affect the conclusions regarding the identification of the carbon pathways in the mechanistic experiments because the changes revealed by those experiments are much larger than the changes between the BASE and the sensitivity experiment.

4. Mechanistic experiments

4.1. MICRO experiment

In the MICRO experiment (Table 3, Fig. 6) the herbivore components of the trophic web (diatoms, nanophytoplankton, carnivorous and omnivorous zooplankton) were removed from the model. The model was run with only the microbial food web active. The absence of a herbivorous chain results in an increase in the available phosphate concentrations compared to the BASE experiment, most probably due to the reduced competition for nutrients. On the other hand, chlorophyll and microzooplankton (microzooplankton and heterotrophic nanoflagellates) concentrations decrease. This result could be due to fewer photosynthetic organisms in the system, which cause both a lower primary production and less prey available for microzooplankton. Despite these system changes, however, the temporal evolution and distribution of concentrations in the water column throughout the year is comparable to that of the BASE experiment. The fact that concentrations and distribution do not greatly differ from the BASE experiment highlights the importance of the microbial trophic web in this area.

4.2. HERB experiment

In the HERB experiment (Table 2, Fig. 6), the simulated trophic web was reduced to the herbivore branch by removing all the microbial functional groups (bacteria, picophytoplankton, microzooplankton and heterotrophic nanoflagellates). To some extent, this configuration simplifies the system by making it a more classical NPZD (nutrients–phytoplankton–zooplankton–detritus) model, where the remineralisation is at a constant rate, substituting the roles of the bacteria and heterotrophic nanoflagellates (Fasham et al., 2000). Organic matter remineralisation was thus computed by introducing a constant remineralisation rate, while the grazing pressure on the primary producers was entirely dependent on the herbivorous mesozooplanktonic group.

The variety of remineralisation rates found in the literature (Table 4) prompted us to carry out various sensitivity runs to test the responsiveness of the BFM to a constant remineralisation rate applied to dissolved and particulate matter. We ran simulations adopting a constant remineralisation parameter of 0.05, 0.1 and 0.2 d^{-1}. The progressive increase in the constant remineralisation parameter always yielded a much higher phytoplankton biomass compared to that obtained in the BASE experiment. The increase was roughly proportional to the increase in the magnitude of the constant remineralisation parameter. Here we show results obtained using a constant remineralisation parameter of 0.1 d^{-1}.

The removal of all the microbial components from the system leads to a decrease in phosphate concentrations, but an increase in ammonium and nitrates. The high nutrient standing stock results in a very strong phytoplankton biomass (diatoms and nanophytoplankton). Very high chlorophyll concentrations (>8 mg Chl-*a* m^{-3}) occur between June and July in the lower part of the water column, close to the seabed. The temporal and

Table 4
Remineralisation rates found in literature.

Author	Year	Remineralisation rate (d^{-1})
Davis and Steele (1994)	1994	0.2
Fasham (1995)	1995	0.05
Doney et al. (1996)	1996	0.1
Stickney et al. (2000)	2000	0.05
Edwards (2001)	2001	0.1
Fennel et al. (2001)	2001	0.05
Lima and Olson (2002)	2002	0.25
Schartau and Oschlies (2003)	2003	0.048
Lima and Doney (2004)	2004	0.2
Powell et al. (2006)	2006	1.03
Fennel et al. (2006)	2006	0.01/0.03
Fiechter et al. (2009)	2009	1.0
Dorman et al. (2011)	2011	0.1
Scott et al. (2011)	2011	0.1
Kriest and Oschlies (2011)	2011	0.05
Kriest et al. (2012)	2012	0.05
Heinle and Slawig (2013)	2013	0.048

spatial distribution of mesozooplankton reflects that of primary production, as expected. This rather different state of the system obtained by forcing the trophic web to be only "herbivorous", appears to depend on the lack of competition for nutrients between primary producers and bacteria, and on the reduced grazing pressure (removal of microzooplankton). Under these conditions, the primary producers underwent a very strong development, with much higher phytoplankton biomass than obtained in the BASE and MICRO experiments. This is also reflected by the concentrations of omnivorous mesozooplankton, which increased dramatically compared to the BASE experiment. These results highlight the importance of the microbial system in controlling the availability of the limiting nutrient via competition.

4.3. BASE × 5 experiment

The BASE × 5 experiment involved a significant change in surface nutrient forcing (concentrations were quintupled) and was designed to test the model's sensitivity to external changes. This is mandatory when developing a management tool, and can also be considered as a first attempt to investigate the response of the ecosystem to coastal eutrophication.

Results of the BASE × 5 experiment are shown in Fig. 6 (bottom row). The enhanced surface nutrient flux boosted the primary production processes, as indicated by the much higher (with respect to the BASE Experiment) chlorophyll concentrations. The strongly increased phytoplankton biomass determined the overall increase in the consumers biomass and the phosphate accumulation near the bottom in summer, as a result of the large organic matter sinking. However, the changes induced by the increased nutrient input are not simply quantitative, but also involve a strong remodulation of the main mass and energy flux through the trophic web. In fact, in order to highlight the outcome of the experiment, several indexes of ecosystem functioning were also considered. Indexes relating to the BASE × 5 experiment were compared to the corresponding indexes from the BASE experiment (Fig. 7) in order to observe system reactions in such conditions. The indexes considered were: the ratio between herbivorous (phytoplankton to zooplankton) and microbial (from bacterioplankton to zooplankton) grazing (Legendre and Rassoulzadegan, 1995), the phosphorus flux between bacteria and phosphate, the ratio between micro–nano phytoplankton and picophytoplankton, and the ratio between meso- and microzooplankton.

The grazing ratio in Fig. 7(A) helps to identify the prevailing trophic web pattern. Index values greater than one indicate a prevailing "herbivorous" trophic web, while values smaller than one indicate a prevailing "microbial" pathway. It should be noted that in the BASE experiment, the trophic structure is persistently "microbial" from May to November, and "herbivorous" for the rest of the year. For a significant part of the year, a larger nutrient input (BASE × 5 experiment) leads to a restructuring of the trophic web thus making it a more "herbivorous" structure, with a shorter and weaker "microbial" period during the warmest months.

The bacterial functional role was also examined via the phosphorus flux between bacteria and phosphate (Fig. 7(B)). In concomitance with a shift in the trophic web structure, the bacterial functional role also changed. Generally speaking, bacteria tend to act as net organic matter remineralizers (positive flux) when the herbivorous trophic web is dominant, and competitors for inorganic phosphorus (negative flux) when microbes prevail. In BASE × 5, this structure was enhanced and the shift in the bacterial roles is very evident. While in the BASE experiment bacteria always acted as phytoplankton competitors (with the flux close to zero during winter months) for nutrients, in BASE × 5, fluxes were stronger and the switch between roles is clear. From December to April bacteria act as remineralizers, with fluxes reaching >0.02 mmol m^{-3} d^{-1}. During warmer months however, they compete with phytoplankton for nutrients. Therefore, higher nutrients concentrations cause the system to shift towards a more herbivorous trophic structure and a more varied bacterial activity.

Phytoplankton and zooplankton ratios (Fig. 7(C) and (D)) give an indication of the size distribution in these communities. Results show how, as a consequence of higher nutrient concentrations in the system, larger phytoplankton and zooplankton groups develop (higher ratios). In fact, it is clear how the more modest nutrient concentrations of the BASE experiment lead to a system mainly composed of smaller organisms.

The results of the BASE × 5 experiment support the theory advanced by Legendre and Rassoulzadegan (1995), that the reduction in the limiting nutrient influences the type of the prevailing food web. This was also found by Thingstad and Sakshaug (1990) in their idealised, steady-state, mathematical model, and by Samuelsson et al. (2002) in their microcosm experiments. Riegman et al. (1993) also found that small algae are better competitors for light and nutrients than larger algae. Thus, the model demonstrated its capability to respond appropriately to nutrient forcing, thus capturing the major food web dynamics.

5. Discussion

5.1. Trophic interactions

The mechanistic experiments were designed to achieve a qualitative understanding of the lower trophic level web dynamics, and of the role played by different functional groups in determining the trophic web structure. The comparison with the available observations indicated that the model is able to capture (within one standard deviation) the observed seasonal dynamics of biogeochemical variables.

The results of the MICRO and HERB experiments highlighted that the importance of the microbial and herbivorous food webs is mostly governed by environmental conditions (Legendre and Rassoulzadegan, 1995; Danger et al., 2007).

When only the microbial web was kept active (MICRO experiment), the vertical structure and the temporal variability of the biogeochemical state variables differed little from the reference simulation (BASE Experiment). On the contrary, concentrations increased unrealistically in the HERB experiment.

Such results confirm the findings of Fonda Umani et al. (2006) about the importance of the microbial food web even in a coastal environment. The microbial food web prevalence appears to be dictated by the nutrient limitation condition as suggested by the

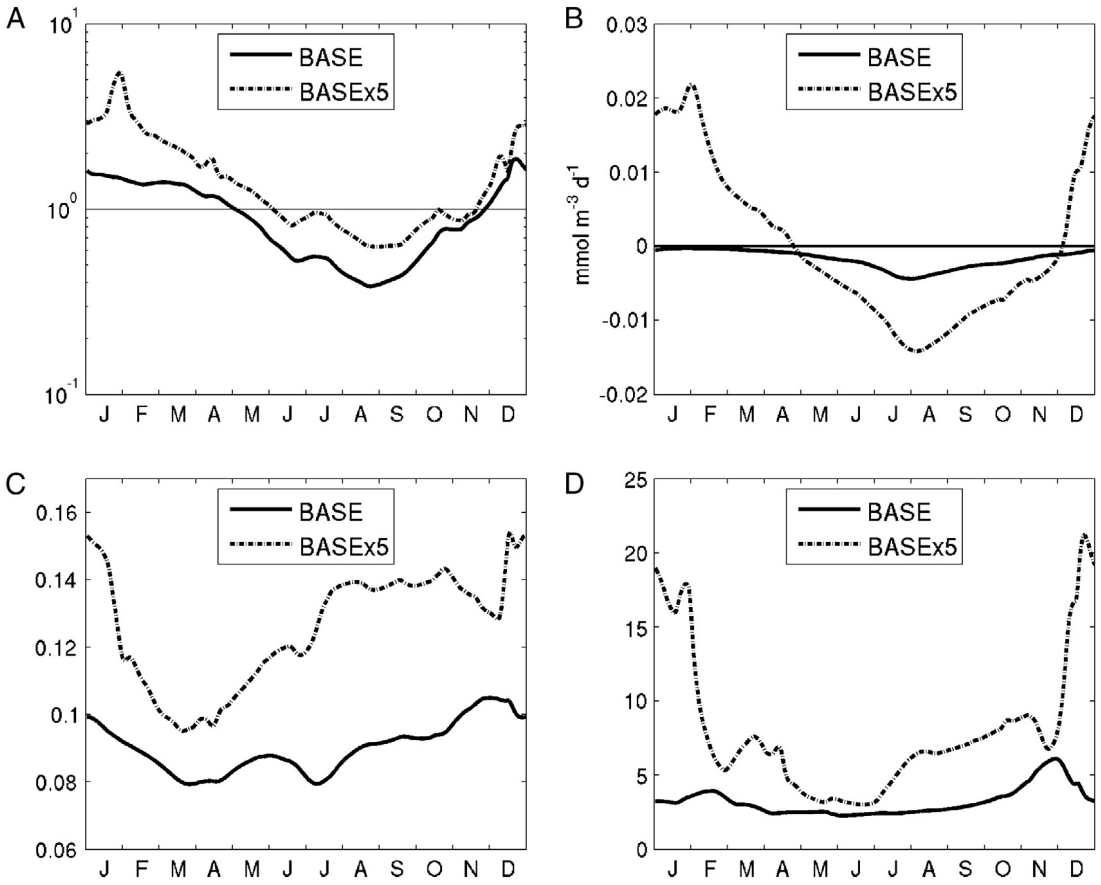

Fig. 7. Indices of ecosystem functioning and matter-transfer pathways. (A) Ratio between the carbon flow due to herbivorous grazing (from autotrophs to zooplankters, values greater than one) and the one due to microbial grazing (from bacterioplankton to zooplankters, values smaller than one; in semi-logarithmic scale). (B) Phosphorus flux between bacteria and dissolved inorganic phosphorus (Positive flux when remineralising, negative flux when competing). (C) Ratio between micro–nano phytoplankton and picophytoplankton. (D) Ratio between omnivorous mesozooplankton and microzooplankton.

BASE × 5 experiment. In fact, the substantial increase of the nutrient external input indicated a shift of the main mass and energy flow through the trophic web. The system responded to the change in the external forcing by shifting from a prevailing microbial structure to an alternating microbial and herbivorous structure. Similarly, Hardman-Mountford et al. (2013) also observed an alteration of the plankton community towards larger organisms in response to surface nutrient enrichment.

These results support the theory advanced by Legendre and Rassoulzadegan (1995), that the reduction in the nutrient limitation conditions influence the type of prevailing food web. This was also found by Thingstad and Sakshaug (1990) in their idealised, steady-state, mathematical model, and by Samuelsson et al. (2002) in their microcosm experiments.

5.2. Management questions addressed

Experiment results demonstrated that the BFM–POM 1D system is able to correctly simulate the lower level trophic interactions and carbon pathways of the Gulf of Trieste.

Furthermore, it proved to be able to modify its main trophic structure in response to changes in the external forcing. From a quantitative point of view, model performance is still relatively low mainly because the Gulf of Trieste physical dynamics is not well captured by a 1-D model which neglects horizontal advection and horizontal patchiness. Thus the study was directed towards a more holistic assessment, focusing on the overall system characteristics rather than on specific state variables. As already stressed above, seasonal structures and trends were generally correctly captured and ecosystem functions were appropriately represented. This opens the way for the use of the model to explore and discover causal relationships (de Mora et al., 2016).

With the increased complexity of marine legislation, the need to have available cost-effective decision tools is urgent in order to understand the state of the environment (Hyder et al., 2015).

We believe that BFM–POM 1D could potentially help in answering some of the questions regarding the Good Environmental Status (GES) under the Marine Strategy Framework Directive (MSFD). In fact, our study addresses, at least partially, questions regarding the interactions between food web structure and other GES descriptors, the impacts of changes in shelf seas biogeochemistry on ecosystem state and the potential efficiency gains from redesigning monitoring programmes.

In particular, BFM–POM 1D can provide information regarding food web structure and eutrophication (descriptors 4 and 5 respectively), which are of particular interest to the MSFD. The model shows to have an overall robust structure (see supplementary material, Appendix C), which is recommended for the study of the low level trophic food web structure. Moreover, experiment BASE × 5 highlighted changes induced by variations on nutrient inputs.

Therefore, a science-based modelling tool, such as the one developed here, could help decision makers to understand lower trophic web interactions in a given area (if backed up by extensive and reliable hydrodynamical data), and to study the sensitivity of the system to external forcings. This could be considered a first step in the definition of a science-based tool, which exploits the structure of a complex biogeochemical model for exploring environmental issues.

5.3. Improvements and future work

Overall, BFM–POM 1D shows some weaknesses in the representation of certain variables such as chlorophyll, oxygen and DOC, which are on the whole underestimated. Similarly, ammonium tends to be overestimated near the seabed. This could be the result of the parametrisation of nitrification, which is not mediated by bacteria.

Future work should be directed towards the inclusion of a fourth phytoplanktonic functional group (large phytoplankton) and a more complete benthic model, rather than a simple benthic return. In such shallow areas, the benthic environment can potentially play a critical role in the carbon cycle dynamics and in shaping the pelagic realm.

Work is currently being carried out in order to satisfy these improvements and further investigate and understand the Gulf of Trieste area.

Acknowledgements

Giulia Mussap was financially supported by the Erasmus Mundus foundation [specific grant agreement number 2011-1614/001-001 EMJD] and wishes to extend her sincere gratitude.

Data originated by Cinzia De Vittor, Dino Viezzoli, Miroslav Gacic, Fabio Brunetti are supplied by OGS as Italian National Oceanographic Data Center/IOC.

Appendix A

The coupled numerical model BFM–POM

The BFM–POM 1D combines the physical with the biological processes to compute the temporal rate of change of a generic biogeochemical variable expressed in terms of concentration $A_j(z, t)$, where $j = 1, 2, 3, \ldots, n_{state}$ and n_{state} corresponds to the total number of pelagic state variables. Tables A.1–A.5 give the specific state variables with the parameters' values used in the equations as written in Vichi et al. (2007). The temporal rate of change of A_j is therefore defined as:

$$\frac{\partial A_j}{\partial t} = \left.\frac{\partial A_j}{\partial t}\right|_{phys} + \left.\frac{\partial A_j}{\partial t}\right|_{bio} \tag{A.1}$$

where the rate of change due to physical processes is defined as

$$\left.\frac{\partial A_j}{\partial t}\right|_{phys} = -W_s \frac{\partial A_j}{\partial z} + \frac{\partial}{\partial z}\left[K_H \frac{\partial A_j}{\partial z}\right]. \tag{A.2}$$

Here, W_s is he settling velocity of the variable, and $W_s = 0$ for the dissolved constituents. K_H is the diffusion coefficient.

The surface boundary conditions are:

$$K_H \left.\frac{\partial A_j}{\partial z}\right|_{z=0} = 0 \tag{A.3}$$

for all the LO and NO state variables type,

$$K_H \left.\frac{\partial A_j}{\partial z}\right|_{z=0} = F_j \tag{A.4}$$

for the (see Table A.1) $O^{(2)}$ (dissolved oxygen), $O^{(3)}$ (carbon dioxide) and $O^{(5)}$ (alkalinity) state variables, where F_j is the flux computed at the air–sea interface according to Wanninkhof (1992).

For the nutrient IO state variables ($N^{(1)}$, $N^{(3)}$, $N^{(4)}$, $N^{(5)}$) the surface boundary condition is:

$$K_H \left.\frac{\partial A_j}{\partial z}\right|_{z=0} = \lambda(A_j - A_{js}) \tag{A.5}$$

where A_j is the current nutrient surface value, A_{js} is the corresponding climatological value and λ is the relaxation velocity (here set to 0.6 m d^{-1}).

At the bottom ($z = -H$) the boundary conditions are:

$$K_H \left.\frac{\partial A_j}{\partial z}\right|_{z=-H} = 0 \tag{A.6}$$

for all LO and NO state variables, while for the IO is:

$$K_H \left.\frac{\partial A_j}{\partial z}\right|_{z=-H} = \omega_{remin} \triangle z_{bot} \tag{A.7}$$

where $\triangle z_{bot}$ is the depth of the bottommost layer of the vertical grid and ω_{remin} is a calculated sediment–water exchange rate at the bottom interface for A_j. This is defined as

$$\omega_{remin} = A_{j_{ben}}\, \alpha_{rmn} \tag{A.8}$$

where $A_{j_{ben}}$ is the concentration of detritus in the benthic environment and α_{rmn} is the specific prescribed remineralisation rate.

Oxygen consumption is stoichiometrically associated to carbon remineralisation rates and the nitrogen remineralisation is partitioned into ammonium and nitrate flux with a constant value. Table A.6 summarises the values used for the concentration of detritus and the remineralisation rates.

Regarding light in the biological model, phytoplankton's self-shading effect is taken into consideration and the irradiance, used as forcing functions for the calculation of production rates, is defined as

$$E_{PAR} = \varepsilon_{PAR} Q_S e^{\lambda_w z + \int_z^0 \lambda_{bio}(z')dz'} \tag{A.9}$$

where ε_{PAR} is the coefficient determining the portion of PAR,

$Q_S e^{\lambda_w z + \int_z^0 \lambda_{bio}(z')dz'}$ is the incoming solar radiation at the surface, λ_w is the visible extinction coefficient and

$$\lambda_{bio} = \sum_i c_{P_i} P_i + c_D D + c_M M \tag{A.10}$$

where P_i is the carbon content of phytoplankton groups in the model, D the carbon content of particulate detritus and M the suspended inorganic sediments (ISM). The c constants are the specific contributions to the total extinction coefficient of each suspended substance (Vichi et al., 2003). Surface PAR is prescribed through daily values means.

The POM

POM is a free surface, hydrostatic, primitive equation, finite difference model (Blumberg and Mellor, 1983). In this "diagnostic" one dimensional implementation, the model prognostically computes the vertical velocity (u, v) and turbulent diffusivity profiles (K_M, K_H) for tracers and momentum. The temperature and salinity (and therefore density) vertical profiles are dynamically interpolated in time from climatological monthly profiles. The prognostic equations for the velocity profiles are:

$$\frac{\partial U}{\partial t} - fV = \frac{\partial}{\partial z}\left(K_M \frac{\partial U}{\partial z}\right) \tag{A.11}$$

$$\frac{\partial V}{\partial t} + fU = \frac{\partial}{\partial z}\left(K_M \frac{\partial V}{\partial z}\right) \tag{A.12}$$

where $f = 2\Omega \sin\phi$ is the Coriolis parameter and ϕ is the latitude. The vertical diffusivity coefficients are calculated assuming the closure hypothesis $K_M(z) = qlS_H$, where S_H is an empirical function (Mellor and Yamada, 1982). The change in time of turbulent kinetic energy is then

$$\frac{\partial}{\partial t}\left(\frac{q^2}{2}\right) = \frac{\partial}{\partial z}\left(K_M \frac{\partial q^2/2}{\partial z}\right) + P_s + P_b - \varepsilon \tag{A.13}$$

where $q^2/2$ is the turbulent kinetic energy, K_M diffusion, P_s the turbulent kinetic energy production by shear, P_b the buoyant production/dissipation and ε the dissipation due to turbulence.

The turbulent length scale is defined as:

$$\frac{\partial}{\partial t}(q^2 l) = \frac{\partial}{\partial z}\left(K_M \frac{\partial q^2 l}{\partial z}\right) + E_1[P_S + P_b] - \frac{q^3}{B_1}\tilde{W} \tag{A.14}$$

where $\tilde{W}$ is a function of the distance between rigid boundaries, and E_1 and B_1 are empirical constants.

Boundary conditions

To solve Eqs. (A.11)–(A.14), we need to define vertical boundary conditions for U, V, q^2, $q^2 l$.

The U and V vertical boundary conditions are:

$$K_M \frac{\partial U}{\partial z}\bigg|_{z=0} = \tau_w^{(x)} \tag{A.15}$$

$$K_M \frac{\partial V}{\partial z}\bigg|_{z=0} = \tau_w^{(y)} \tag{A.16}$$

$$K_M \frac{\partial \vec{U}}{\partial z}\bigg|_{z=-H} = \vec{\tau}_b \tag{A.17}$$

where $\vec{\tau}_w = (\tau_w^{(x)}, \tau_w^{(y)})$ is the wind stress prescribed through interpolation between adjacent monthly values and $\vec{\tau}_b$ is the bottom drag coefficient defined as

$$\vec{\tau}_b = C_b \left|\vec{U}_b\right| \vec{U}_b \tag{A.18}$$

where C_b is the bottom drag coefficient, and $\vec{U}_b = (U_b, V_b)$ is the velocity at the bottommost layer.

The boundary conditions for turbulent kinetic energy at the surface ($z = 0$) depend on the wind stress intensity and are represented by the following semi-empirical equation:

$$q^2\Big|_{z=0} = B_1^{\frac{2}{3}} \frac{|\vec{\tau}_w|}{C_d}. \tag{A.19}$$

The bottom boundary condition ($z = -H$) is

$$q^2\Big|_{z=-H} = B_1^{\frac{2}{3}} \frac{|\vec{\tau}_b|}{C_b}. \tag{A.20}$$

Appendix B

Description and values of the parameters of BFM–POM 1D used in the BASE experiment. The parameter choice originates from a calibration exercise carried out based on model defaults, Vichi et al. (2007) and personal communication.

Table A.1
List of the reference state variables A_i for the pelagic model. The subscript i indicates the basic components (if any) of the variable, e.g. $P_i^{(1)} \equiv (P_c^{(1)}, P_n^{(1)}, P_p^{(1)}, P_s^{(1)}, P_l^{(1)}, P_f^{(1)})$.

n_{state}	Variable	Type	Const.	Units	Description
1	$N^{(1)}$	IO	P	mmolP m^{-3}	Phosphate
2	$N^{(3)}$	IO	N	mmolN m^{-3}	Nitrate
3	$N^{(4)}$	IO	N	mmolN m^{-3}	Ammonium
4	$N^{(5)}$	IO	Si	mmolSi m^{-3}	Silicate
5	$N^{(6)}$	IO	R	mmolS m^{-3}	Reduction equivalents, HS^-
6	$O^{(2)}$	IO	O	mmolO_2 m^{-3}	Dissolved oxygen
7	$O^{(3)}$	IO	C	mgC m^{-3}	Carbon dioxide
8	$O^{(5)}$	IO	–	mmol Eq m^{-3}	Total alkalinity
9	$P_i^{(1)}$	LO	C N P Si Chl	mgC m^{-3}, mmolN–P m^{-3}, µmol, mg Chl-*a* m^{-3}	Diatoms
10	$P_i^{(2)}$	LO	C N P Chl	mgC m^{-3}, mmolN–P m^{-3}, µmol, mg Chl-*a* m^{-3}	Flagellates
11	$P_i^{(3)}$	LO	C N P Chl	mgC m^{-3}, mmolN–P m^{-3}, µmol, mg Chl-*a* m^{-3}	Picophytoplankton
12	$P_i^{(4)}$	LO	C N P Chl	mgC m^{-3}, mmolN–P m^{-3}, µmol, mg Chl-*a* m^{-3}	Picophytoplankton
13	B_i	LO	C N P	mgC m^{-3}, mmolN–P m^{-3}	Pelagic bacteria
14	$Z_i^{(3)}$	LO	C N P	mgC m^{-3}, mmolN–P m^{-3}	Carnivorous mesozooplankton
15	$Z_i^{(4)}$	LO	C N P	mgC m^{-3}, mmolN–P m^{-3}	Omnivorous mesozooplankton
16	$Z_i^{(5)}$	LO	C N P	mgC m^{-3}, mmolN–P m^{-3}	Microzooplankton
17	$Z_i^{(6)}$	LO	C N P	mgC m^{-3}, mmolN–P m^{-3}	Heterotrophic Flagellates
18	$R_i^{(1)}$	NO	C N P	mgC m^{-3}, mmolN–P m^{-3}	Labile dissolved organic matter
19	$R_c^{(2)}$	NO	C	mgC m^{-3}	Semi-labile dissolved organic carbon
20	$R_i^{(3)}$	NO	C	mgC m^{-3}	Semi-refractory dissolved organic carbon
21	$R_i^{(6)}$	NO	C N P Si	mgC m^{-3}, mmolN–P–Si m^{-3}	Particulate organic detritus

Legend: IO = Inorganic; LO = Living organic; NO = Non-living organic.

Table A.2
List of the parameters in the BFM pelagic equations for phytoplankton.

Parameter	Symbol	$P^{(1)}$	$P^{(2)}$	$P^{(3)}$
Characteristic Q10 coefficient (–)	p_q10	2.0	2.0	2.0
Cut-off threshold for temperature factor (–)	p_qtemp	0.0	0.0	0.0
Maximal productivity at 10 °C (day^{-1})	p_sum	2.5	3.0	3.5
Respiration rate at 10 °C (day^{-1})	p_srs	0.05	0.05	0.05
Max.specific nutrient-stress lysis rate (day^{-1})	p_sdmo	0.01	0.01	0.01
Half saturation constant for nutrient stress lysis (–)	p_thdo	0.1	0.1	0.1

(continued on next page)

Table A.2 (*continued*)

Parameter	Symbol	$P^{(1)}$	$P^{(2)}$	$P^{(3)}$
Extra lysis rate (biomass density-dependent) (day^{-1})	p_seo	0.0	0.0	0.0
Half saturation constant for extra lysis ($mgC\ m^{-3}$)	p_sheo	0.0	0.0	0.0
Excreted fraction of primary production (–)	p_pu_ea	0.01	0.1	0.1
Activity respiration fraction (–)	p_pu_ra	0.1	0.1	0.2
Membrane affinity for N (m^3/mgC/day)	p_qun	0.025	0.025	0.025
Half saturation constant for NH_4 uptake preference over NO_3 ($mmolN/m^3$)	p_lN4	1.0	0.5	0.1
Minimum quotum N:C (mmolN/mgC)	p_qnlc	6.87×10^{-5}	6.87×10^{-5}	6.87×10^{-5}
Reference quotum N:C (mmolN/mgC)	p_qncPPY	0.0126	0.0126	0.0126
Multiplication factor for luxury storage (–)	p_xqn	2.0	2.0	2.0
Membrane affinity for P (m^3/mgC/day)	p_qup	2.5×10^{-3}	2.5×10^{-3}	2.5×10^{-3}
Minimum quotum P:C (mmolP/mgC)	p_qplc	4.29×10^{-4}	4.29×10^{-4}	4.29×10^{-4}
Reference quotum P:C (mmolP/mgC)	p_qpcPPY	7.86×10^{-4}	7.86×10^{-4}	7.86×10^{-4}
Multiplication factor for luxury storage (–)	p_xqp	2.0	2.0	2.0
Half saturation conc. for dissolved Si limitation ($mmolSi\ m^{-3}$)	p_chPs	1.0	0.0	0.0
Membrane affinity for Si (m^3/mgC/day)	p_qus	0.0	0.0	0.0
Minimum quotum Si:C (mmolSi/mgC)	p_qslc	4.3×10^{-3}	0.0	0.0
Reference quotum Si:C (mmolSi/mgC)	p_qscPPY	8.5×10^{-3}	0.0	0.0
Nutrient stress threshold for sinking (–)	p_esNI	0.7	0.75	0.75
Maximum Sinking velocity ($m\ day^{-1}$)	p_res	5.0	0.5	0.5
Specific turnover rate for Chla (day^{-1})	p_sdchl	0.2	0.2	0.2
Initial slope of the P-E curve ($mgC\ s\ m^2$/mgChl/uE)	p_alpha_chl	1.1×10^{-5}	0.46×10^{-5}	0.7×10^{-5}
Reference quotum Chla:C (mgChla/mgC)	p_qlcPPY	0.035	0.02	0.02
Chla-specific extinction coefficient (m^2/mgChla)	p_epsChla	0.03	0.03	0.03
Relaxation rate towards maximum Chla:C (day^{-1})	p_tochl_relt	0.25	0.25	0.25
Optimal value of E_PAR/E_K (–)	p_EpEk_or	3.0	3.0	3.0

Table A.3
List of the parameters in the BFM pelagic equations for microzooplankton.

Parameter	Symbol	$Z^{(5)}$	$Z^{(6)}$
Q10 value for physiological rates (–)	p_q10	2.0	2.0
Potential growth rate (day^{-1})	p_sum	2.0	5.0
Respiration rate at 10 °C (day^{-1})	p_srs	0.02	0.02
Mortality rate due to oxygen limitation (day^{-1})	p_sdo	0.25	0.25
Temperature independent mortality (day^{-1})	p_sd	0.0	0.0
Assimilation efficiency (–)	p_pu	0.5	0.3
Fraction of activity excretion (–)	p_pu_ea	0.25	0.35
Half-saturation oxygen concentration ($mmolO_2\ m^{-3}$)	p_chro	0.5	0.5
Half-saturation food concentration for Type II ($mgC\ m^{-3}$)	p_chuc	200.0	200.0
Half-saturation food concentration for preference factor ($mgC\ m^{-3}$)	p_minfood	50.0	50.0
Maximum quotum N:C (mmolN/mgC)	p_qncMIZ	1.67×10^{-2}	1.67×10^{-2}
Maximum quotum P:C (mmolN/mgC)	p_qpcMIZ	1.85×10^{-3}	1.85×10^{-3}

Table A.4
List of the parameters in the BFM pelagic equations for mesozooplankton.

Parameter	Symbol	$Z^{(3)}$	$Z^{(4)}$
Q10 value for physiological rates (–)	p_q10	2.0	2.0
Respiration rate at 10 °C (day^{-1})	p_srs	0.01	0.02
Potential growth rate (day^{-1})	p_sum	2.0	2.0
Specific search volume ($m^3\ mgC\ d^{-1}$)	p_vum	0.0025	0.0025
Assimilation efficiency (–)	p_puI	0.6	0.6
Fraction of faeces production (–)	p_peI	0.3	0.35
Specific density-dependent mortality ($m^3\ mgC\ d^{-1}$)	p_sdo	0.01	0.01
Background natural mortality (day^{-1})	p_sd	0.02	0.01
Exponent of density-dependent mortality (–)	p_sds	2.0	2.0
Maximum quotum P:C (mmolP/mgC)	p_qpcMEZ	1.67×10^{-3}	1.67×10^{-3}
Maximum quotum N:C (mmolN/mgC)	p_qncMEZ	0.015	0.015
Half-saturation O_2 concentration ($mmolO_2\ m^{-3}$)	p_clO2o	30.0	30.0

Table A.5
Pelagic bacteria parameters description and value.

Parameter	Symbol	$B^{(1)}$
Characteristic Q10	p_q10	2.95
Half saturation constant for O_2 ($mmol/m^3$)	p_chdo	30.0
Specific mortality rate (day^{-1})	p_sd	0.0
Density dependent specific mortality rate (day^{-1})	p_sd2	0.0
Specific potential uptake fro nutrient-rich DOM (day^{-1})	p_suhR1	0.5
Specific potential uptake fro nutrient-poor DOM (day^{-1})	p_sulR1	0.0
Specific potential uptake for semi-labile DOC (day^{-1})	p_suR2	0.05

(continued on next page)

Table A.5 (*continued*)

Parameter	Symbol	$B^{(1)}$
Specific potential uptake for semi-refractory DOC (day^{-1})	p_suR3	0.01
Specific potential uptake for POM (day^{-1})	p_suR6	0.1
Specific potential growth rate (day^{-1})	p_sum	8.38
Activity respiration fraction (–)	p_pu_ra	0.4
Additional respiration fraction at low O_2 (–)	p_pu_ra_o	0.2
Specific rest respiration (day^{-1})	p_srs	0.01
Optimal N/C ratio (mmolN/mgC)	p_qncPBA	0.0167
Optimal P/C ratio (mmolP/mgC)	p_qpcPBA	0.00185
Minimal N/C ratio (mmolN/mgC)	p_qlnc	0.0167
Minimal P/C ratio (mmolP/mgC)	p_qlpc	0.00095
Membrane affinity for N (mmolN/mgC/day)	p_qun	0.05
Membrane affinity for P (mmolP/mgC/day)	p_qup	0.005
Half saturation ammonium conc. for uptake ($mmolN/m^3$)	p_chn	5.0
Half saturation ammonium conc. for uptake ($mmolP/m^3$)	p_chp	0.5
Relaxation timescale for N uptaken/remin. (day^{-1})	p_ruen	1.0
Relaxation timescale for P uptaken/remin. (day^{-1})	p_ruep	1.0
Relaxation timescale for semi-labile excretion (day^{-1})	p_rec	1.0
Excretion of semi-refractory DOC (–)	p_pu_ea_R3	0.015

Table A.6
Pelagic food matrix.

Predators	Preys							
	$P_i^{(1)}$	$P_i^{(2)}$	$P_i^{(3)}$	$Z_i^{(3)}$	$Z_i^{(4)}$	$Z_i^{(5)}$	$Z_i^{(6)}$	$B_i^{(1)}$
$Z_i^{(3)}$	0.0	0.0	0.0	1.0	1.0	1.0	0.0	0.0
$Z_i^{(4)}$	1.0	0.75	0.7	0.0	1.0	1.0	0.0	0.0
$Z_i^{(5)}$	1.0	1.0	0.1	0.0	0.0	1.0	1.0	0.1
$Z_i^{(6)}$	0.0	0.2	1.0	0.0	0.0	0.0	0.2	1.0

Table A.7
Benthic nutrient concentrations, remineralisation rates and partitioning coefficient.

Symbol	Value	Units	Description
$p\_reminQ_c^{(6)}$	0.005	d^{-1}	Specific remineralisation rate of carbon
$p\_reminQ_n^{(6)}$	0.005	d^{-1}	Specific remineralisation rate of nitrate
$p\_reminQ_p^{(6)}$	0.005	d^{-1}	Specific remineralisation rate of phosphate
$p\_reminQ_s^{(6)}$	0.005	d^{-1}	Specific remineralisation rate of silicate
p_pQIN3	0.1	–	Partitioning coefficient between NO_3 and NH_4

Appendix C. Supplementary material

Supplementary material related to this article can be found online at http://dx.doi.org/10.1016/j.rsma.2016.03.015.

References

Azam, Farooq, Long, Richard A., 2001. Oceanography: Sea snow microcosms. Nature 414 (6863), 495–498.

Baretta, J.W., Ebenhoh, W., Ruardij, P., 1995. The European regional seas ecosystem model, a complex marine ecosystem model. Neth. J. Sea Res. (ISSN: 0077-7579) 33 (3–4), 233–246. http://dx.doi.org/10.1016/0077-7579(95)90047-0.

Berrisford, Paul, Dee, D., Fielding, K., Fuentes, M., Kallberg, P., Kobayashi, S., Uppala, S., 2009. The era-interim archive. Technical report. ECMWF, Shinfield Park, Reading.

Bianchi, D., Zacatarelli, M., Pinardi, N., Capozzi, R., Capotondi, L., Corselli, C., Masina, S., 2006. Simulations of ecosystem response during sapropel s1 depositton event. Palaeogeogr. Palaeoclimatol. Palaeoecol. 235.

Blumberg, Alan F., Mellor, George L., 1983. Diagnostic and prognostic numerical circulation studies of the south atlantic bight. J. Geophys. Res.: Oceans (ISSN: 2156-2202) 88 (C8), 4579–4592. http://dx.doi.org/10.1029/JC088iC08p04579.

Blumberg, Alan F., Mellor, George L., 1987. A Description of a Three-Dimensional Coastal Ocean Circulation Model. American Geophysical Union, ISBN: 9781118665046, p. 208. http://dx.doi.org/10.1029/CO004p0001.

Butenschon, Momme, Zavatarelli, Marco, Vichi, Marcello, 2012. Sensitivity of a marine coupled physical biogeochemical model to time resolution, integration scheme and time splitting method. Ocean Modell. (ISSN: 1463-5003) 52–53 (0), 36–53. http://dx.doi.org/10.1016/j.ocemod.2012.04.008.

Curtin, Richard, Prellezo, Raúl, 2010. Understanding marine ecosystem based management: A literature review. Mar. Policy (ISSN: 0308-597X) 34 (5), 821–830. http://dx.doi.org/10.1016/j.marpol.2010.01.003.

Danger, Michael, et al., 2007. Control of phytoplankton–bacteria interactions by stoichiometric constraints. Oikos 116 (7), 1079–1086.

Davis, Cabell S., Steele, John H., 1994. Biological/physical modeling of upper ocean processes. Technical report. Woods Hole Oceanographic Institution.

de Mora, L., Butenschon, M., Allen, J.I., 2016. The assessment of a global marine ecosystem model on the basis of emergent properties and ecosystem function: a case study with ERSEM. Geosci. Model Develop. 9 (1), 59–76. http://dx.doi.org/10.5194/gmd-9-59-2016.

Doney, Scott C., 2010. The growing human footprint on coastal and open-ocean biogeochemistry. Science 328 (5985), 1512–1516.

Doney, Scott C., Glover, David M., Najjar, Raymond G., 1996. A new coupled, one-dimensional biological-physical model for the upper ocean: Applications to the {JGOFS} bermuda atlantic time-series study (bats) site. Deep Sea Res. Part II (ISSN: 0967-0645) 43 (2–3), 591–624. http://dx.doi.org/10.1016/0967-0645(95)00104-2.

Dorman, Jeffrey G., Powell, Thomas M., Sydeman, William J., Bograd, Steven J., 2011. Advection and starvation cause krill (euphausia pacifica) decreases in 2005 northern california coastal populations: Implications from a model study. Geophys. Res. Lett. (ISSN: 1944-8007) 38 (4), http://dx.doi.org/10.1029/2010GL046245.

Edwards, Andrew M., 2001. Adding detritus to a nutrient–phytoplankton–zooplankton model:a dynamical-systems approach. J. Plankton Res. 23 (4), 389–413. http://dx.doi.org/10.1093/plankt/23.4.389.

Fasham, M.J.R., 1995. Variations in the seasonal cycle of biological production in subarctic oceans: A model sensitivity analysis. Deep-Sea Res. I (ISSN: 0967-0637) 42 (7), 1111–1149. http://dx.doi.org/10.1016/0967-0637(95)00054-A.

Fasham, M.J.R., Ducklow, H.W., McKelvie, S.M., 2000. A nitrogen-based model of plankton dynamics in the oceanic mixed layer. J. Mar. Res. 48, 591–639. 1990-08-01T00:00:00.

Fennel, Katja, Losch, Martin, Schröter, Jens, Wenzel, Manfred, 2001. Testing a marine ecosystem model: sensitivity analysis and parameter optimization. J. Mar. Syst. (ISSN: 0924-7963) 28 (1–2), 45–63. http://dx.doi.org/10.1016/S0924-7963(00)00083-X.

Fennel, Katja, Wilkin, John, Levin, Julia, Moisan, John, O'Reilly, John, Haidvogel, Dale, 2006. Nitrogen cycling in the middle atlantic bight: Results from a three-dimensional model and implications for the north atlantic nitrogen budget. Glob. Biogeochem. Cycles (ISSN: 1944-9224) 20 (3), http://dx.doi.org/10.1029/2005GB002456.

Fiechter, Jerome, Moore, Andrew M., Edwards, Christopher A., Bruland, Kenneth W., Lorenzo, Emanuele Di, Lewis, Craig V.W., Powell, Thomas M., Curchitser, Enrique N., Hedstrom, Kate, 2009. Modeling iron limitation of primary production in the coastal gulf of alaska. Deep Sea Res. Part II (ISSN: 0967-0645) 56 (24), 2503–2519. http://dx.doi.org/10.1016/j.dsr2.2009.02.010. Physical and Biological Patterns, Processes, and Variability in the Northeast Pacific.

Fonda Umani, Serena, Beran, Alfred, 2003. Seasonal variations in the dynamics of microbial plankton communities: first estimates from experiments in the gulf of trieste, northern adriatic sea. Mar. Ecol. Prog. Ser. 247, 1–16.

Fonda Umani, Serena, et al., 2006. Major inter-annual variations in microbial dynamics in the Gulf of Trieste (northern Adriatic Sea) and their ecosystem implications. Aquat. Microb. Ecol. 46 (2), 163–175.

Giordani, P., Hammond, D.E., Berelson, W.M., Montanari, G., Poletti, R., Milardi, A., Frignani, M., Langone, L., Ravaioli, M., Rovatti, G., Rabbi, E., Vollenweider, R.A., Marchetti, R., Viviani, R., 1992. Benthic fluxes and nutrient budgets for sediments in the northern adriatic sea: burial and recycling efficiencies. Sci. Total Environ. (ISSN: 0048-9697) 251–275. eng.

Guarnieri, A., Pinardi, N., Oddo, P., Bortoluzzi, G., Ravaioli, M., 2013. Impact of tides in a baroclinic circulation model of the adriatic sea. J. Geophys. Res.: Oceans (ISSN: 2169-9291) 118 (1), 166–183.

Hardman-Mountford, N.J., Polimene, L., Hirata, T., Brewin, R.J.W., Aiken, J., 2013. Impacts of light shading and nutrient enrichment geo-engineering approaches on the productivity of a stratified, oligotrophic ocean ecosystem. J. Roy. Soc. Interface 10 (89), 20130701. http://dx.doi.org/10.1098/rsif.2013.0701.

Heinle, A., Slawig, T., 2013. Internal dynamics of NPZD type ecosystem models. Ecol. Modell. (ISSN: 0304-3800) 254 (0), 33–42. http://dx.doi.org/10.1016/j.ecolmodel.2013.01.012.

Hyder, K., Rossberg, A.G., Allen, J.I., Austen, M.C., Barciela, R.M., Bannister, H.J., Blackwell, P.G., Blanchard, J.L., Burrows, M.T., Defriez, E., Dorrington, T., Edwards, K.P., Garcia-Carreras, B., Heath, M.R., Hembury, D.J., Heymans, J.J., Holt, J., Houle, J.E., Jennings, S., Mackinson, S., Malcolm, S.J., McPike, R., Mee, L., Mills, D.K., Montgomery, C., Pearson, D., Pinnegar, J.K., Pollicino, M., Popova, E.E., Rae, L., Rogers, S.I., Speirs, D., Spence, M.A., Thorpe, R., Turner, R.K., van der Molen, J., Yool, A., Paterson, D.M., 2015. Making modelling count - increasing the contribution of shelf-seas community and ecosystem models to policy development and management. Marine Policy 61, 291–302. http://dx.doi.org/10.1016/j.marpol.2015.07.015.

Kiørboe, Thomas, 2008. A Mechanistic Approach to Plankton Ecology. Princeton University Press.

Kourafalou, Vassiliki H., 1999. Process studies on the po river plume, north adriatic sea. J. Geophys. Res.: Oceans (ISSN: 2156-2202) 104 (C12), 29963–29985. http://dx.doi.org/10.1029/1999JC900217.

Kriest, I., Oschlies, A., 2011. Numerical effects on organic-matter sedimentation and remineralization in biogeochemical ocean models. Ocean Modell. (ISSN: 1463-5003) 39 (3–4), 275–283. http://dx.doi.org/10.1016/j.ocemod.2011.05.001.

Kriest, I., Oschlies, A., Khatiwala, S., 2012. Sensitivity analysis of simple global marine biogeochemical models. Glob. Biogeochem. Cycles (ISSN: 1944-9224) 26 (2), http://dx.doi.org/10.1029/2011GB004072.

Legendre, Louis, Rassoulzadegan, Fereidoun, 1995. Plankton and nutrient dynamics in marine waters. Ophelia 41 (1), 153–172. http://dx.doi.org/10.1080/00785236.1995.10422042.

Lima, Ivan D., Doney, Scott C., 2004. A three-dimensional, multinutrient, and size-structured ecosystem model for the north atlantic. Glob. Biogeochem. Cycles (ISSN: 1944-9224) 18 (3), http://dx.doi.org/10.1029/2003GB002146.

Lima, Ivan D., Olson, Donald B., Doney, Scott C., 2002. Intrinsic dynamics and stability properties of size-structured pelagic ecosystem models. J. Plankton Res. (ISSN: 0142-7873) 24 (6), 533–556. http://dx.doi.org/10.1093/plankt/24.6.533.

Malacic, V., Petelin, B., 2009. Climatic circulation in the Gulf of Trieste (northern Adriatic). J. Geophys. Res.- Oceans (ISSN: 0148-0227) 114, http://dx.doi.org/10.1029/2008JC004904.

Mellor, G.L., Yamada, T., 1982. Development of a turbulence closure model for geophysical fluid problems. Rev. Geophys. Space Phys. 20 (C2), 851–875.

Mozetic, Patricija, Solidoro, Cosimo, Cossarini, Gianpiero, Socal, Giorgio, Precali, Robert, France, Janja, Bianchi, Franco, De Vittor, Cinzia, Smodlaka, Nenad, Umani, Serena Fonda, 2010. Recent trends towards oligotrophication of the northern adriatic: evidence from chlorophyll a time series. Estuaries Coasts 33 (2), 362–375.

Mozetic, P., Umani, S.F., Cataletto, B., Malej, A., 1998. Seasonal and inter-annual plankton variability in the Gulf of Trieste (northern Adriatic). Ices J. Mar. Sci. (ISSN: 1054-3139) 55 (4), 711–722. http://dx.doi.org/10.1006/jmsc.1998.0396. ICES Symposium on Temporal Variability of Plankton and their Physico-Chemical Environment, KIEL, GERMANY, MAR 19-21, 1997.

Powell, Thomas M., Lewis, Craig V.W., Curchitser, Enrique N., Haidvogel, Dale B., Hermann, Albert J., Dobbins, Elizabeth L., 2006. Results from a three-dimensional, nested biological-physical model of the California Current System and comparisons with statistics from satellite imagery. J. Geophys. Res.- Oceans J. (ISSN: 0148-0227) 111 (C7), http://dx.doi.org/10.1029/2004JC002506.

2012. Regional Environmental Agency, ARPA-FVG. Regional plan on the safeguard of the watershed—analisi conoscitiva.

Riegman, Roel, Kuipers, Bouwe R., Noordeloos, Anna A.M., Witte, Harry J., 1993. Size-differential control of phytoplankton and the structure of plankton communities. Neth. J. Sea Res. (ISSN: 0077-7579) 31 (3), 255–265.

Samuelsson, Kristina, Berglund, Johnny, Haecky, Pia, Andersson, Agneta, 2002. Structural changes in an aquatic microbial food web caused by inorganic nutrient addition. Aquat. Microb. Ecol. 29 (1), 29–38.

Schartau, Markus, Oschlies, Andreas, 2003. Simultaneous data-based optimization of a 1d-ecosystem model at three locations in the north atlantic: Part i; method and parameter estimates. J. Mar. Res. 61 (6), 765–793. http://dx.doi.org/10.1357/002224003322981147.

Scott, V., Kettle, H., Merchant, C.J., 2011. Sensitivity analysis of an ocean carbon cycle model in the north atlantic: an investigation of parameters affecting the air-sea co_2 flux, primary production and export of detritus. Ocean Sci. 7 (3), 405–419. http://dx.doi.org/10.5194/os-7-405-2011.

Stickney, H.L., Hood, R.R., Stoecker, D.K., 2000. The impact of mixotrophy on planktonic marine ecosystems. Ecol. Modell. (ISSN: 0304-3800) 125 (2–3), 203–230. http://dx.doi.org/10.1016/S0304-3800(99)00181-7.

Tedesco, L., Socal, G., Bianchi, F., Acri, F., Veneri, D., Vichi, M., 2007. Nw adriatic sea biogeochemical variability in the last 20 years (1986–2005). Biogeosciences 4 (4), 673–687.

Thingstad, T.F., Sakshaug, E., 1990. Control of phytoplankton growth in nutrient recycling ecosystems. theory and terminology. Mar. Ecol. Prog. Ser. 63, 261–272.

Vichi, M., Oddo, P., Zavatarelli, M., Coluccelli, A., Coppini, G., Celio, M., Umani, S.F., Pinardi, N., 2003. Calibration and validation of a one-dimensional complex marine biogeochemical flux model in different areas of the northern Adriatic shelf. Ann. Geophys. (ISSN: 0992-7689) 21 (1, Part 2), 413–436.

Vichi, M., Pinardi, N., Masina, S., 2007. A generalized model of pelagic biogeochemistry.for the global ocean ecosystem. Part I: Theory. J. Mar. Syst. (ISSN: 0924-7963) 64 (1–4), 89–109. http://dx.doi.org/10.1016/j.jmarsys.2006.03.006. Symposium on Advances in Marine Ecosystem Modelling Research, Plymouth, ENGLAND, JUN 27-29, 2005.

Wanninkhof, Rik, 1992. Relationship between wind speed and gas exchange over the ocean. J. Geophys. Res.: Oceans (ISSN: 2156-2202) 97 (C5), 7373–7382.

Zavatarelli, M., Pinardi, N., Kourafalou, V.H., Maggiore, A., 2002. Diagnostic and prognostic model studies of the Adriatic Sea general circulation: Seasonal variability. J. Geophys. Res.- Oceans (ISSN: 0148-0227) 107 (C1), http://dx.doi.org/10.1029/2000JC000210.